UK Atomic Energy Authority

ExCALIBUR

NEPTUNE: Options for Geometry Representation

Milestone M2.1.1

Abstract

This report describes work for ExCALIBUR project NEPTUNE at Milestone 2.1.1. Investigation of high order mesh generation using for example Nekmesh as an optimal strategy for representing fusion device geometry in the presence of strong anisotropy induced by the magnetic field.

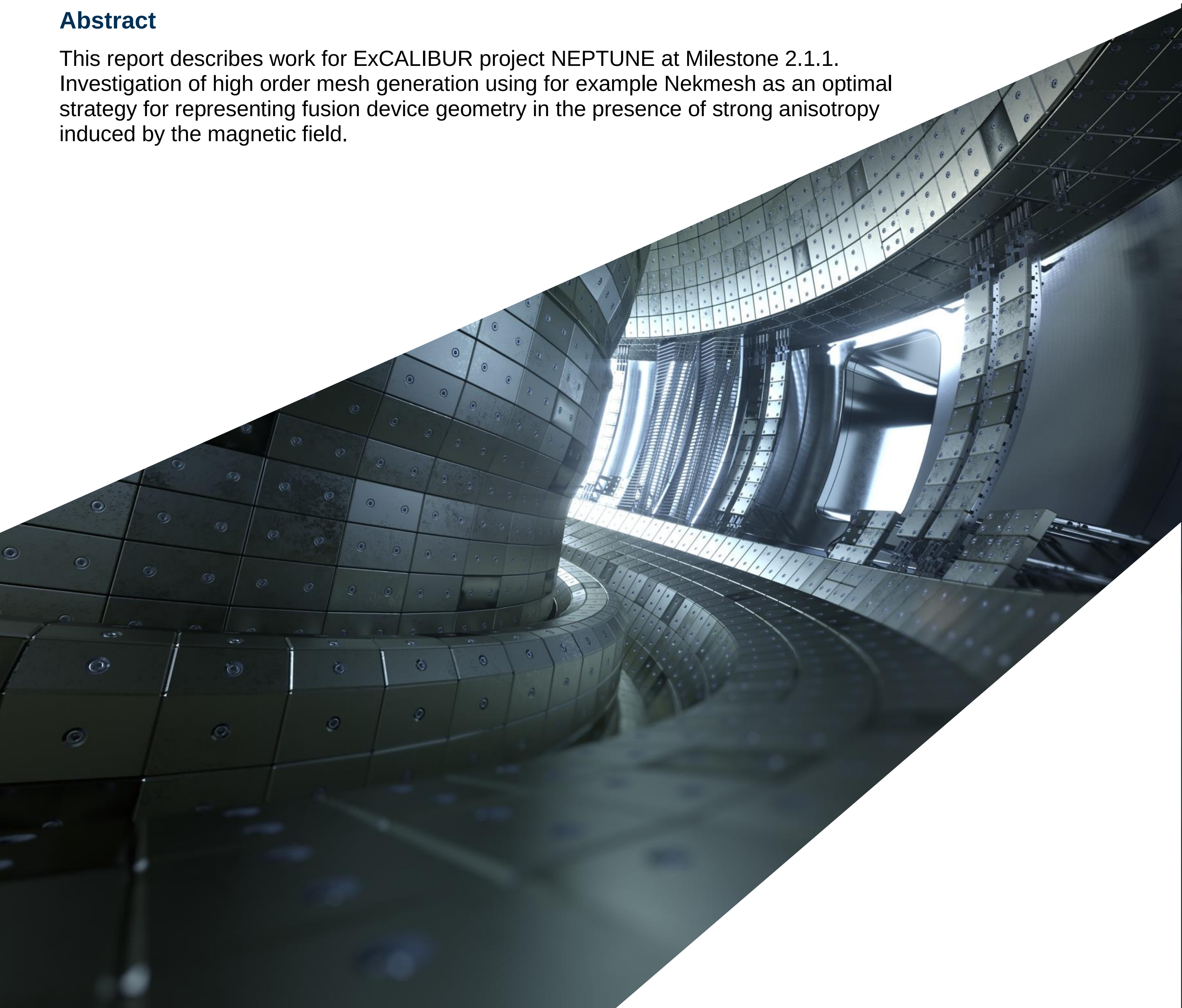

UKAEA REFERENCE AND APPROVAL SHEET

	Client Reference:	
	UKAEA Reference:	CD/EXCALIBUR-FMS/0012
	Issue:	1.00
	Date:	10 March 2020

Project Name: ExCALIBUR Fusion Modelling System.

Version 1.00

	Name and Department	Signature	Date
Prepared By:	Wayne Arter Lucian Anton Debasmita Samaddar	N/A N/A N/A	10/03/2020 10/03/2020 10/03/2020
Reviewed By:	Rob Akers	N/A	10/03/2020
Modified By:	Rob Akers MSSC		10/03/2020
Approved By:	Rob Akers MSSC		12/03/2020

NEPTUNE: Options for Geometry Representation

Contents

Chapter 1

Introduction

1.1 Target Geometry

Figure 1.1 indicates the complexity of the designed geometry of the ITER tokamak interior. Figure 1.2 shows an image of an existing device (in this case JET), together with simplified CAD to the right (the complexity of ITER and DEMO first wall geometry is expected to be similar to JET). The ITER wall is covered with Berilium tiles, there are ducts entering from the right (shown blanked off), grilles protecting antennas, and the divertor chamber at the bottom, with exposed support structures in some designs. All these features may have to be dealt with by a SOL (Scrape Off Layer) code as they can be impacted by both plasma and neutral gas. Further, in order to gain full benefit from the use of spectral element schemes, the exterior of this geometry, viz. the interior of the device, needs to be meshed using elements which conform to the surfaces to a correspondingly high order of accuracy.

An important practical point is the representation of 3-D geometry to a SOL code. With existing design techniques, the interior will have been produced using a CAD system such as CATIA^{TM}. The geometry then needs to be discretised for the code to be able to model it, usually by separate software that produces a mesh starting with the CAD and additional metadata. A complete specification, part made in the CAD package will have labels describing the materials of the different surfaces (also important to future edge physics simulation doe to sputtering and complex chemical processes at the interface between plasma and materials). A modeller will want to add metadata specifying boundary conditions, describing the meshes and other aspects of the discretisations to be applied in different regions or on different surfaces, etc.

1.2 CAD

To understand meshing, it is therefore necessary to understand how ‘CAD’ works. By ‘CAD’ we mean the way the geometry (primarily) of objects is represented and stored on computers, *not* the process (Computer Aided Design) by which it is produced. Modern Computer Aided Design systems work ‘bottom up’, so that a design may in fact start with a set of points. These points are then used to generate curves and the curves in turn are used to define surfaces, leading to the so-called B-rep, or boundary representation of geometry. Earlier CAD systems however worked directly with a simple set of canonical bodies such as half-spaces, cylinders and spheres, which could be rotated, translated and combined by Boolean set operations to give the CSG (constructive solid geometry) representation of the physical object.

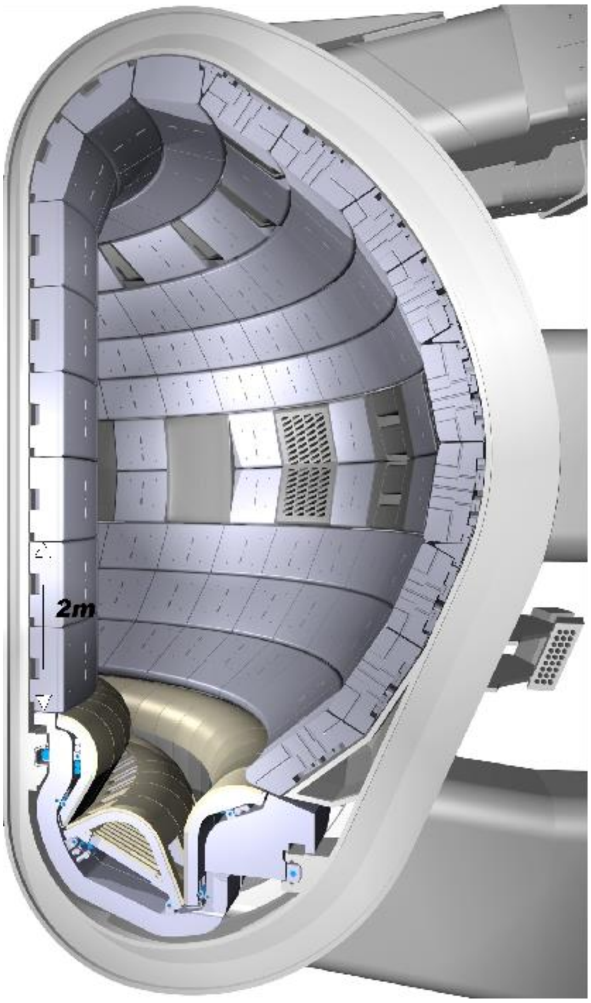

Figure 1.1: The complexity of the ITER first wall

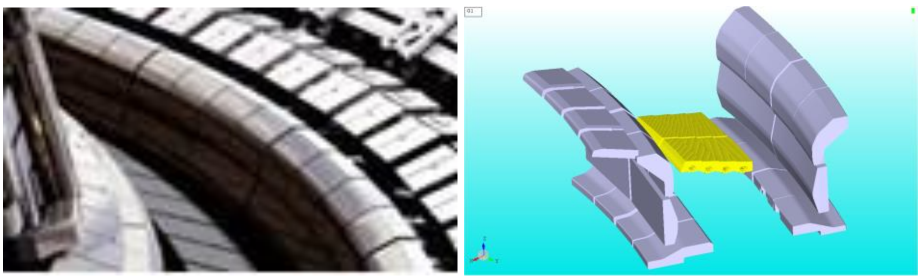

Figure 1.2: Close-up of the JET divertor showing individual tiles (left) and simplified CAD representation (right).

The B-rep approach uses NURBS to represent curves and hence also surfaces, where

NURBS are mathematically complex objects. NURBS stands for nonuniform rational B-splines [1]. The 'non-uniform' and 'B' aspects are technicalities which need not be gone into, but clearly the spline property is important in that it ensures curves are smooth. 'Rational' is important because it means that the representation uses rational polynomials, so that if quadratic NURBS are used, the conic sections (e.g. ellipses) can be exactly represented. To illustrate this feature of quadratic NURBS, recall that the unit circle ($x^2 + y^2 = 1$) may be written as

$$x = \frac{(1-t^2)}{(1+t^2)}; \qquad y = \frac{2t}{(1+t^2)} \qquad (1.1)$$

It may correspondingly be shown [1] that cubic NURBS allow an exact representation of all the quadric surfaces (eg. ellipsoids and cones).

An important kind of 'B' spline is the Bezier spline. This is constructed by successive splitting of chords as illustrated in Figure 1.3 for the case of a quadratic (non-rational) Bezier spline.

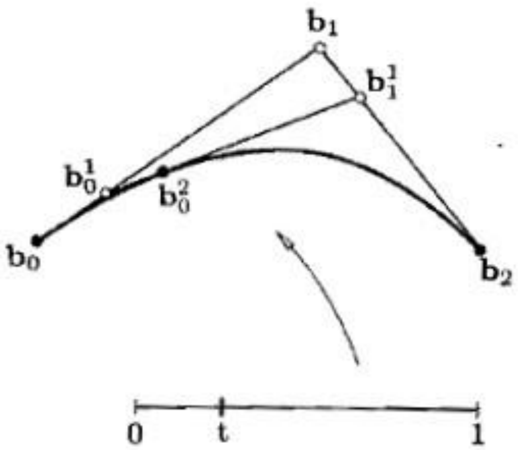

Figure 1.3: Construction of a quadratic Bezier spline, taken from ref [1]. The point on the curve parameterised by t is produced by splitting each of the lines b_0b_1 and b_1b_2 in the ratio t : (1 − t), then splitting the line joining the new points in the same proportion.

NURBS are preferred because of their greater flexibility in the ability to generate smooth surfaces. The flexibility comes at a price however, which may be paid when two quite distinct NURBS surfaces need to be joined - so-called 'trimmed NURBS'. There are no simple mathematical formulae to determine NURBS surface intersection, and so recourse has to be made to some kind of approximation. In practice what may be done is to consider the intersection curve as the definitive, independent 3-D object. This however will not lie exactly on either NURBS surface, each of which becomes more of a guide than a definition of where the surface lies as the bounding curves are approached. Alternatively the trim curves may be defined in terms of the surface parameters, either as short line segments or as parametric NURBS, but then each surface at the join will have a slightly different ‘intersection’ curve.

Even when topological information *is* stored such as in the STEP or other proprietary formats, the use of approximation in surface intersection, in combination with round-off error, can still lead to the appearance of small “spurious” features. There may be genuine small features in a CAD database, e.g. small pipework, rivet heads and other fasteners. For many codes these may not be important and are undesirable because by increasing the number of objects to be modelled - they also increase the code running time. Thus, the first problem to be treated by a CAD interface is to remove both spurious and genuine small geometrical features by ‘CAD repair and defeaturing’. An indication of the size of this problem is that this was the principal aim of the CADfix™ software which represents many man-years of development effort. Even with modern software tools and the results of years of research, to replicate this software from scratch would be expected to take man-years. Finally at the end of this process, there is a consistent B-rep ready for meshing.

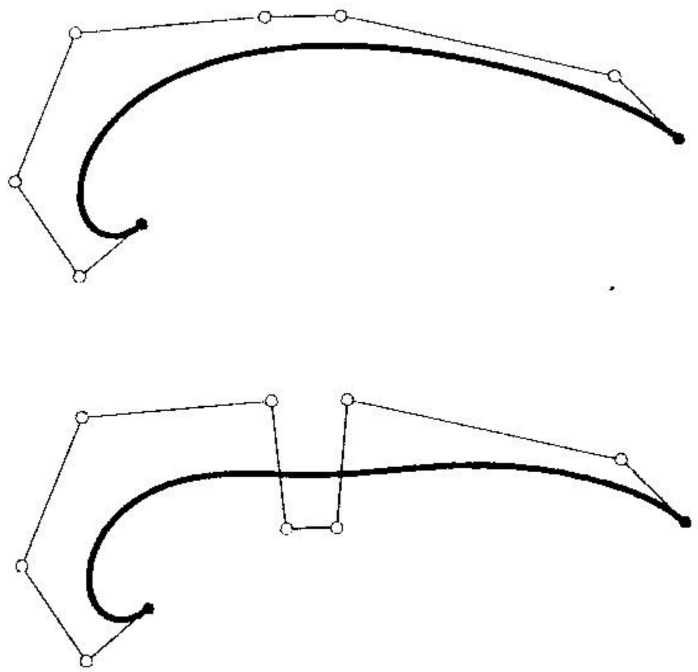

Figure 1.4: How CAD is often produced, taken from ref [1]. The designer moves two of the control points, shown as open circles, to shape the curve.

Chapter 2

Task Work

There are two basic approaches to meshing a B-rep, namely (1) to represent the geometry by means of ‘voxels’ [2], or (2) to mesh the surface, then generate a volume mesh that coincides with the surface mesh.

Voxels are the volume equivalent of pixels, so that the geometry is represented by a uniform cuboid lattice of geometrically identical cells, each possibly labelled with a set of physical properties. Refinements of voxelisation are to allow clusters of small cells to be treated as larger cuboid bodies [3], and to omit cells altogether within say solid surfaces (also known as ‘tartan meshing’). When both techniques are combined in say CFD, the result is known as an AMR mesh, see Figure 2.1.

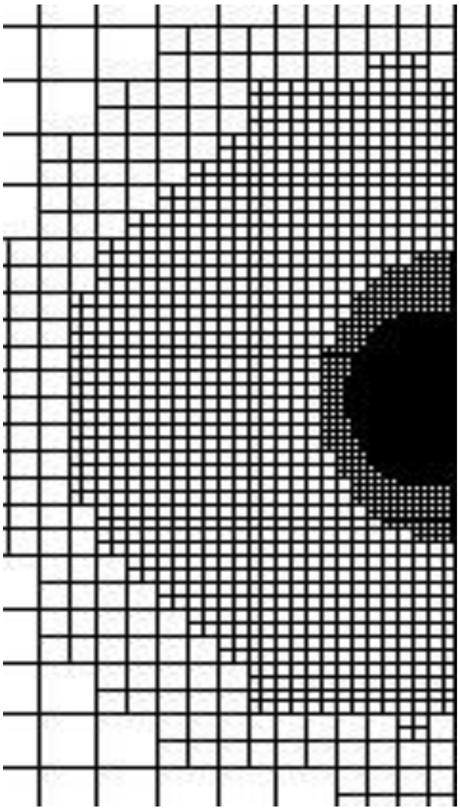

Figure 2.1: An AMR mesh surrounding a curved body drawn as solid black at right.

As suggested by the previous paragraph, an AMR mesher is potentially quite complicated. A well-known difficulty with schemes that use AMR meshes is illustrated by Figure 2.2 for a light propagation problem. There will be interfaces between meshes of different size, even in regions with the same physical properties. However, a wave with a wavelength of less than $10h$, where h is the local mesh-spacing, modelled using a second-order accurate scheme, has a propagation speed in error by 1%, which error increases as h^p typically with p = 2. Thus computationally, the region show in Figure 2.2 may have different dispersion properties at shorter wavelength in the two different grid-sizes, and computations will exhibit a spurious reflection at the interface, which may be misleading or even destabilising in certain cases. The importance of the work of Nikiforakis et al [4] is that they have managed to produce in effect a spatio-temporal AMR mesh, so that they can compute the equations of inviscid compressible FD *explicitly* using a local timestep. Such meshes have also been successfully used for Particle-in-Cell calculations of extreme complexity for spacecraft charging [5], meaning that Nikiforakis work deserved attention. Unfortunately, considerable discussion of the merits of the Nikiforakis approach versus spectral element at the Feb 5th ExCALIBUR NEPTUNE community workshop in Birmingham [6] indicated potentially severe difficulties for AMR meshes when diffusion, especially anisotropic diffusion has to be treated.

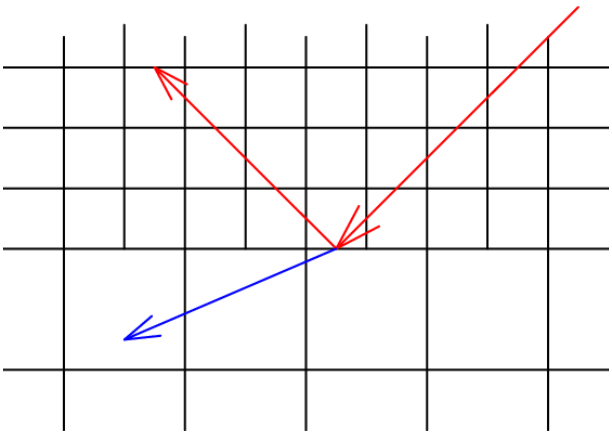

Figure 2.2: Spurious reflections when using a low order scheme with AMR.

2.1 Importance of Geometrical Accuracy

The approximate nature of the intersection between two NURBS surfaces may also cause difficulties, as indicated by Figure 2.3. Power deposition on the plasma fascing components (PFCs) shielding may depend critically upon the direction of the surface normal. A grid of planar triangles may produce errors like those indicated by Figure 2.3(a), whereas more faithful representations would resemble Figure 2.3(b).

A difficulty for both AMR and surface-based approaches is the order of error p_s in the spatial approximation of surfaces and other interfaces used to bound the domain of a PDE calculation. The important result is by Boffi [7] that the results of a PDE calculation can have order no higher than p_s. Thus in the usual approach that starts by meshing the surface with simple planar triangles, there is no point in using schemes of high or spectral order. Many meshing packages allow only for second order surface approximations, whereby typically each side of say a ‘curved’ triangle is represented by three points and hence a quadratic fit. A notable exception is gmsh [8].

Extensive consultations as part of the Y1 ExCALIBUR NEPTUNE Requirements Capture indicate difficulties with higher-order spatially accurate meshing even for relatively simple geometries that might be encountered in the tokamak edge. Figure 2.4 shows two problems. The first is where self-intersection occurs when trying to insert nodes inside thin elements near curved boundaries. The other is where the surface triangulation has a tangency to an extrusion. We have determined that the Nekmesh software is being developed [9, 10] using concepts from optimisation theory to treat such issues.

(a)
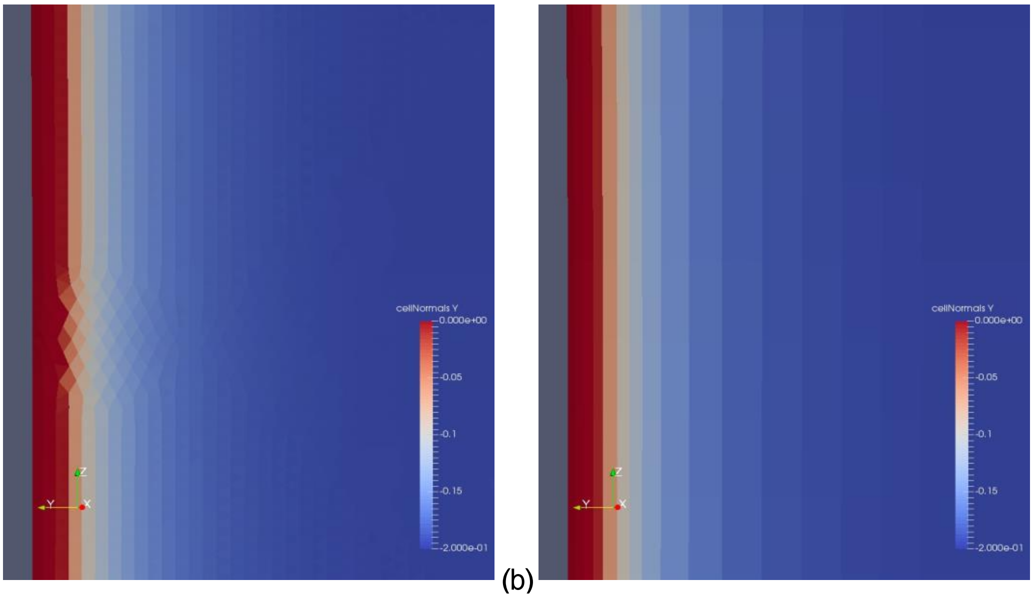

(b)

Figure 2.3: Close-ups of two triangular meshes of the central left edge surface of a TBM (Test Blanket Module) Tungsten shield. The CAD contains a join in the middle of the image leading to the irregular behaviour of the horizontal component of surface normal in the image at left (a). Refitting of CAD using the CADfix™ software package enables the production of a more smoothly varying normal, see mesh at right (b).

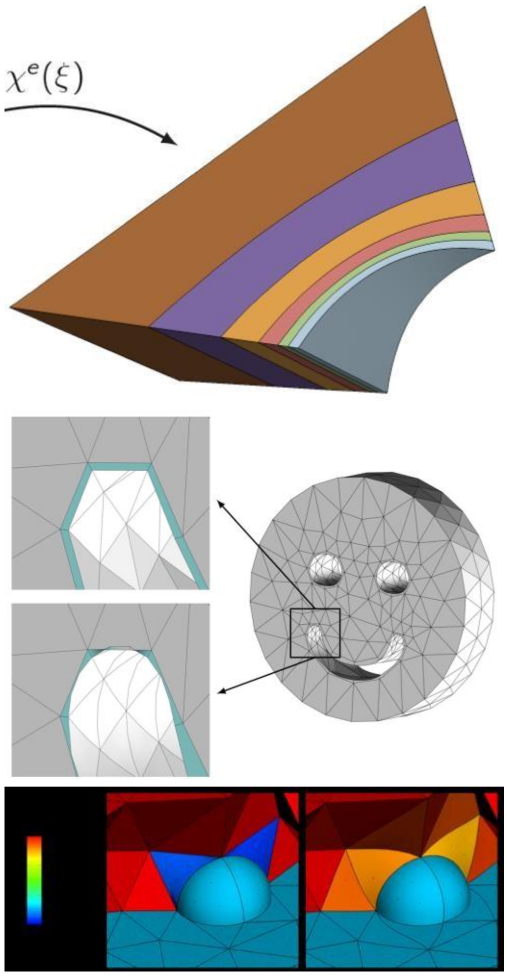

Figure 2.4: At top is illustrated a desirable meshing close to a curved surface, when eg. small scale physical effects due to a sheath need to be represented. Below is an indication of how packages may fail when they try to produce this mesh using low-order spatially spatially accurate elements (planar triangles), from a presentation by Sherwin and Moxey at CCFE. At bottom is a second picture from the same presentation, showing resolution of a problem arising when mesh is tangent to a surface.

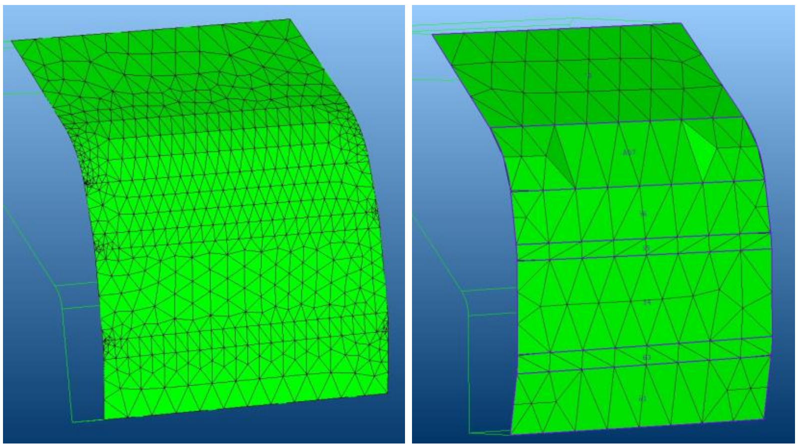

Figure 2.5: Different T1 meshes produced with (left) and without sag control (right). The left plot has mesh features illustrating the gap between bounding NURBS curve and NURBS surface, caused in this case by defeaturing of fillets around the surface edges.

2.2 Example Meshing Problem

An example test case has been formed by the meshing of the surface of JET Tile 1 (T1), one of the vertical tiles at the left of the divertor in Figure 1.2. The figures containing surface meshes are taken from a study in ref [RP4,§5.1][11] that attempted to find a minimal, accurate mesh representation for the T1 surfaces receiving power.

A sample test case using Nekmesh is illustrated in Figure 2.7 for the JET Tile 1, which is one of the vertical tiles at the left of the divertor in Figure 1.2.

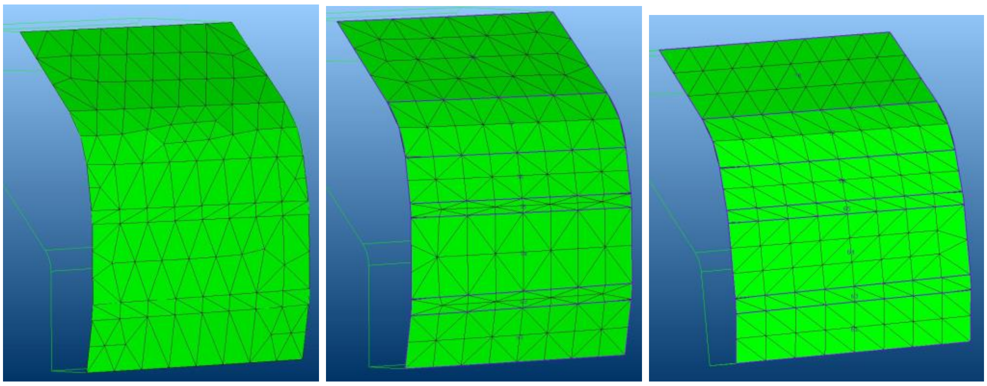

Figure 2.6: Exploration of the effect of different meshing controls on T1.

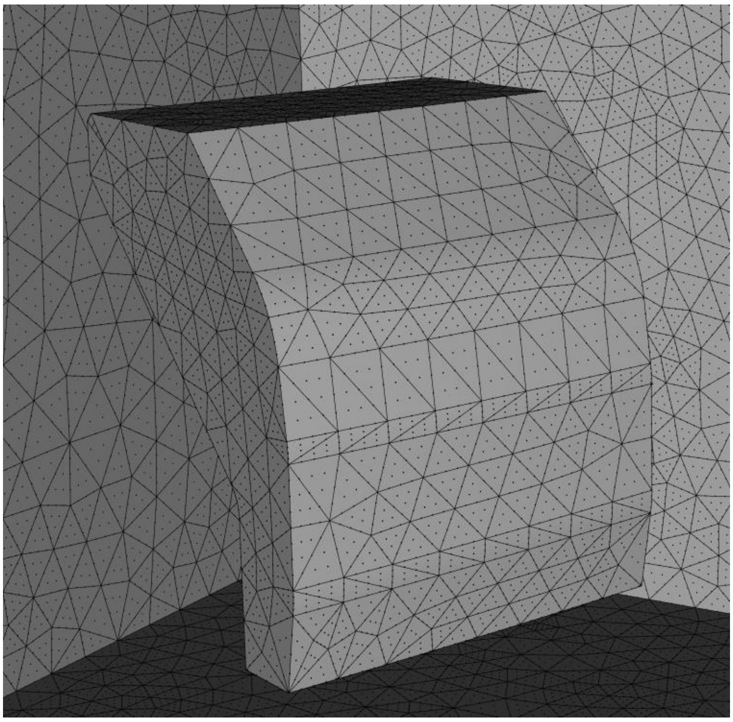

Figure 2.7: Meshing of JET T1 tile by D. Moxey 6/3/20 using Nekmesh. The dots indicate nodes within the non-planar triangular elements.

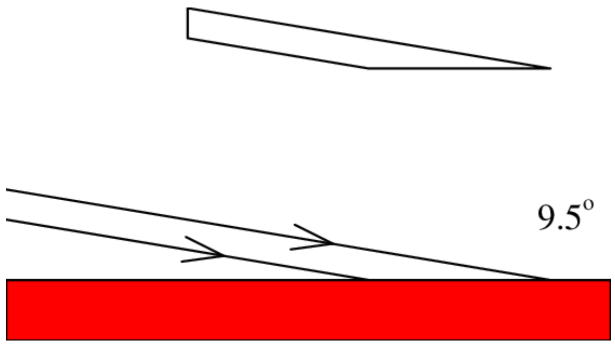

Figure 2.8: Undesirable element shape if meshing conforms to both surface and fieldline.

2.3 Element Shape Problem

Even assuming accurate meshing, there is a problem caused by the need to spread power as widely as possible over the surfaces. Power is observed to flow along field lines, being deposited proportionately as $\hat{\boldsymbol{n}}.\hat{\boldsymbol{B}}$ where $\hat{\boldsymbol{n}}$ is the unit normal to the surface and $\hat{\boldsymbol{B}}$ gives the direction of magnetic field $\mathbf{B}$. Many designs call for a $2\ \mathrm{degree}$ angle of field incidence on the surface. Such a small angle is hard to draw, so we show an angle of $9.5\ \mathrm{degrees}$ $(\arctan 1/6)$ - see Figure 2.8. Elements with $2\ \mathrm{degree}$ corners (or less) present such serious challenges that simultaneous alignment with both the fieldlines and the geometry appears to be a non-starter. The Science Plan [12] recognises that it will be important to establish just how large an anisotropy in the transport can be treated accurately without special coding.

Chapter 3

Summary

As discussed in the Year One Summary Report [13], spectral elements are desirable on grounds of accuracy. Consideration and discussions have indicated that the accuracy of the spectral element approach can be maintained in complex geometries provided surfaces are meshed to a sufficiently high degree of accuracy. Producing such meshes can be challenging, but recent developments (Nekmesh) based around the spectral/hp element library Nektar++ are showing promise that these challenges can be met. We conclude therefore that resource should be directed to ensuring that this emergent capability can handle PFC and other geometries relevant to the tokamak edge.

Acknowledgement

The support of the UK Meteorological Office and Strategic Priorities Fund is acknowledged.

Bibliography

[1] G. Farin. *Curves and surfaces for computer aided geometric design*. Academic Press Professional, Inc. San Diego, CA, USA, 1990, 5th Edition 2002.

[2] K.W. Burn, C. Daffara, G. Gualdrini, M. Pierantoni, and P. Ferrari. Treating voxel geometries in radiation protection dosimetry with a patched version of the Monte Carlo codes MCNP and MCNPX. *Radiation Protection Dosimetry*, 123(3):345–353, 2007.

[3] K.A. Van Riper and O. Journals. A CT and MRI scan to MCNP input conversion program. *Radiation Protection Dosimetry*, 115(1-4):513–516, 2005.

[4] N. Gokhale, N. Nikiforakis, and R. Klein. A dimensionally split cartesian cut cell method for hyperbolic conservation laws. *Journal of Computational Physics*, 364:186–208, 2018.

[5] Y Miyake and H Usui. Particle-in-cell modeling of spacecraft-plasma interaction effects on double-probe electric field measurements. *Radio Science*, 51(12):1905–1922, 2016.

[6] D. Samaddar. Report on Y1 2019 Internal Workshop. Technical Report CD/EXCALIBUR-FMS/0018-1.00-M1.1.1a, UKAEA, 2020. Report on Y1 2020 External Workshop (REPORT1). Technical Report CD/EXCALIBUR-FMS/0010-1.00-M1.1.1b, UKAEA, 2020.

[7] L. Botti. Influence of reference-to-physical frame mappings on approximation properties of discontinuous piecewise polynomial spaces. *Journal of Scientific Computing*, 52(3):675–703, 2012. http://dx.doi.org/10.1007/s10915011-9566-3.

[8] C. Geuzaine and J.-F. Remacle. Gmsh: A 3-d finite element mesh generator with built-in pre-and post-processing facilities. *International journal for numerical methods in engineering*, 79(11):1309–1331, 2009.

[9] M. Turner, D. Moxey, J. Peiro, M. Gammon, C.R. Pollard, and H. Buck-´ low. A framework for the generation of high-order curvilinear hybrid meshes for CFD simulations. *Procedia Engineering*, 203:206–218. http://dx.doi.org/10.1016/j.proeng.2017.09.808.

[10] M. Turner, J. Peiro, and D. Moxey.´ Curvilinear mesh generation using a variational framework. *Computer-Aided Design*, 103:73–91, 2018. https://doi.org/10.1016/j.cad.2017.10.004.

[11] W. Arter, D. Calleja, H. Leggate, and L. Richiusa. Optimising Fieldline Following Software. Technical Report UKAEA-CCFE-RE(19)04,
CCFE, 2019. http://www.ccfe.ac.uk/assets/Documents/ UKAEA-CCFE-RE(19)04.pdf.

[12] W. Arter, L. Anton, D. Samaddar, and R. Akers. ExCALIBUR Fusion Modelling System Science Plan. Technical Report CD/EXCALIBUR-FMS/0001, UKAEA, 2019.

[13] W. Arter, L. Anton, and D. Samaddar. Year One Summary Report. Technical Report CD/EXCALIBUR-FMS/0011-1.00-M1.2.1, UKAEA, 2020.